Superconductivity with broken time-reversal symmetry in ion-irradiated Ba$_{0.27}$K$_{0.73}$Fe$_2$As$_2$ single crystals

V. Grinenko,[1,2,*] P. Materne,[1] R. Sarkar,[1] H. Luetkens,[3] K. Kihou,[4] C. H. Lee,[4] S. Akhmadaliev,[5] D. V. Efremov,[2]
S.-L. Drechsler,[2] and H.-H. Klauss[1]

[1]*Institute for Solid State Physics, TU Dresden, 01069 Dresden, Germany*
[2]*IFW Dresden, Helmholtzstrasse 20, 1069 Dresden, Germany*
[3]*Laboratory for Muon Spin Spectroscopy, PSI, CH-5232 Villigen PSI, Switzerland*
[4]*National Institute of Advanced Industrial Science and Technology (AIST), Tsukuba, Ibaraki 305-8568, Japan*
[5]*Helmholtz-Zentrum Dresden-Rossendorf, 01314 Dresden, Germany*

Over the past years a lot of theoretical and experimental effort has been made to find states with broken time-reversal symmetry (BTRS) in multiband superconductors. In particular, it was proposed theoretically that in the Ba$_{1-x}$K$_x$Fe$_2$As$_2$ system either an $s + is$ or an $s + id$ BTRS state may exist at high doping levels in a narrow region of the phase diagram. Here we report the observation of an enhanced zero-field muon spin-relaxation rate below the superconducting transition temperature for a high quality crystalline sample with $x \approx 0.73$. This indicates that indeed the time-reversal symmetry is broken in superconducting Ba$_{1-x}$K$_x$Fe$_2$As$_2$ at this doping level.

The possibility to change the order parameter symmetry by charge doping in Fe-based superconductors recently attracted considerable attention. At the optimal doping level most of the experimental and theoretical studies suggest an $s_\pm$ superconducting (SC) order parameter symmetry caused by commensurate spin fluctuations between hole and electron Fermi pockets [1]. However, for high doping levels the available results are controversial. In the Ba$_{1-x}$K$_x$Fe$_2$As$_2$ system close to $x = 1$ some of the experimental data were interpreted in favor of s-wave superconductivity [2–6], and others support d-wave superconductivity [7–11]. According to theoretical model calculations [12–14], these states are almost degenerate at the high hole doping level. However, the predicted $s_\pm$ state close to $x = 1$ is qualitatively different from the $s_\pm$ state at optimal doping. For the former the order parameter changes sign between hole pockets [15,16]. Indeed, various experimental investigations indicate that an essential change in the SC and the normal-state properties occur at a K doping of $x \sim 0.7$. Close to this doping level the electron pockets disappear, and only the hole pockets remain on the Fermi surface according to angle-resolved photoemission spectroscopy measurements [17]. Inelastic neutron-scattering measurements revealed that the relation between superconducting transition temperature (T_c) and incommensurability δ of the low-energy spin-fluctuation spectra changes its behavior abruptly around this doping level [18]. At the same time, the spin-resonance energy in the SC state falls below 2Δ between $x = 0.7$ and 0.8, where Δ is the SC gap amplitude. Specific heat investigations show that the behavior of the specific heat jump (ΔC) at the superconducting transition T_c versus T_c deviates from the universal Bud'ko-Ni-Canfield scaling around $x = 0.7$ [19,20]. Additionally, the thermal conductivity at low temperatures changes its behavior from exponential to linear between $x = 0.7$ and 0.8, suggesting the presence of accidental line nodes on some Fermi-surface pockets [4].

It was shown theoretically that the evolution of the order parameter with K doping can occur through intermediate $s + is$ or $s + id$ SC states that possess an arbitrary phase on different Fermi-surface sheets [15,16,21–28]. In both states the time-reversal symmetry is broken, and in the presence of nonmagnetic defects spontaneous currents may emerge [22,23]. An $s + id$ state leads to local currents at any impurities below T_c [29], whereas an $s + is$ state only induces local currents around impurities which locally break the tetragonal symmetry of the lattice [22,23,25,26]. Previous zero-field (ZF) muon spin rotation (μSR) investigations of polycrystalline Ba$_{1-x}$K$_x$Fe$_2$As$_2$ samples with doping levels of $x = 0.5$, 0.6, 0.7, 0.8, and 0.9 did not reveal any noticeable enhancement of the muon spin-relaxation rate below T_c [30]. These results exclude an $s + id$ and possibly an $s + is$ state at these doping levels since in a real material some of the crystalline defects, such as dislocations and grain surfaces, break the C_4 symmetry of the lattice. However, a broken time-reversal symmetry (BTRS) state could be overlooked in this paper since it can occupy a very narrow region in the phase diagram. Moreover, nonmagnetic disorder can narrow or even eliminate the region with a BTRS state since the $s_\pm$ superconductivity is sensitive to nonmagnetic interband impurity scattering [31]. Therefore, experiments with single crystals with disorder under control are necessary to identify the intrinsic phase diagram of the Ba$_{1-x}$K$_x$Fe$_2$As$_2$ system.

In our experiments, we focused on the doping region close to $x = 0.7$ where the SC order parameter may change its symmetry according to various experimental observations. Additionally, we used a low fluence ion irradiation to add a small amount of the symmetry-breaking defects in high quality single crystals. Therefore, we target to detect a BTRS SC state, irrespective of the order parameter symmetry, by its local magnetic fields reflecting the local currents around defects or impurities. We observed that the ZF muon spin-relaxation rate is enhanced below the temperature of $T^* \sim 10$ K, which is lower than $T_c \sim 13$ K for the sample with the doping level of $x \approx 0.73$. However, this behavior is absent for the samples

_____
*v.grinenko@ifw-dresden.de

with $x \approx 0.70$. The temperature dependence of the relaxation rate for $x \approx 0.73$ is consistent with theoretical predictions for both $s + is$ or $s + id$ SC states, whereas its small value points to an $s + is$ rather than an $s + id$ state.

μSR experiments on the stacks of the $Ba_{1-x}K_xFe_2As_2$ single crystals with doping levels of $x = 0.70(2)$ and $0.73(2)$ were performed at the GPS instrument of the πM3 beamline at the Paul Scherrer Institute (PSI) in Villigen, Switzerland. Fully spin-polarized positive muons with an energy of 4.2 MeV were implanted in the sample (parallel to the crystallographic c axis) where they rapidly thermalize and stop at interstitial lattice sites at a depth on the order of 100 μm depending on the sample density. Given that it is very difficult to grow thick enough $Ba_{1-x}K_xFe_2As_2$ single crystals in this doping range suitable for μSR experiments, we used stacks of several platelike (10–50-μm-thick) single crystals with a total thickness of $\sim$200 μm and an area between 3×3 and 4×4 mm^2. To ensure that the muons stop in the sample, we used an Al degrader with a thickness of $d_{Al} = 300$ μm. This value of d_{Al} is sufficient to reduce the muon energy to a value that all muons stop in the sample but not in the Al degrader. The whole assembly was wrapped into a very thin 5-μm Al foil and attached by a thin polyester tape to the Cu sample holder having the form of a fork. The Cu fork is designed in such a way that the muons do not hit the Cu holder. ZF and transverse-field (TF) measurements were performed for two muon polarization modes. In the transverse polarization mode the so-called up-down positron counters were used. The muon spin polarization P_μ is at about 45° with respect to the muon beam (pointing toward the upward counter) and sample c axis [32]. In the longitudinal polarization mode with P_μ antiparallel to the muon momentum (parallel to the sample c axis) the backward and forward counters were used. The data were analyzed using the MUSRFIT software package [33].

The single crystals of two doping levels used in the experiments were selected from a single batch to ensure a similar sample quality. The T_c of each single crystal was checked by magnetization measurements using a commercial superconducting quantum interference device magnetometer from Quantum Design. The single crystals, which had T_c values within 1 K, were used to assemble the crystals' stacks of each doping level. This T_c variation corresponds to 1% to 2% of the doping difference between crystals in the samples used for the experiments. The susceptibility data of the stacks in the SC state are shown below (see Fig. 3 right axes). The doping level was determined by x-ray diffraction using the known dependence of the c-axis lattice constant versus K doping (see Fig. 3 in Ref. [34] and Fig. S1 in the Supplemental Material [35]). The investigated single crystals have a high residual resistivity ratio of $RRR \approx 55$ measured before the irradiation (see Fig. S2 in the Supplemental Material [35]) and a low amount of magnetic impurities indicated by the negligibly small upturn in the temperature dependence of the normal-state magnetic susceptibility (Fig. 1). A low fluence of $\sim 10^{10}$ cm^2 of I^{+9} ions with an energy of $\sim$50 MeV with an angle of 60° with respect to the single-crystal ab plane was used to irradiate the samples. Each thin single crystal was irradiated from both sides to ensure that a large sample volume contains irradiation defects. Such an ion beam produces columnar defects (see Fig. 1 in Ref. [36]), which, in
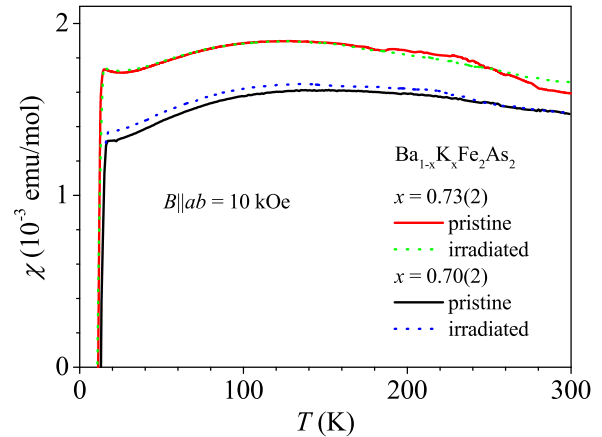

FIG. 1. Temperature dependence of the molar susceptibility χ_m of the $Ba_{1-x}K_xFe_2As_2$ single-crystal stacks used in μSR experiments measured before (solid curves) and after (dashed curves) ion irradiation.

our case, are nonsymmetrical on the ab plane. These defects locally break the tetragonal C_4 symmetry of the lattice and, as predicted, should induce currents for both $s + is$ and $s + id$ symmetries. As one can see in Fig. 3, the irradiation did not affect T_c since the distance between defects of about 100 nm is much larger than the SC coherence length $\xi_{ab} = \Phi_0/2\pi H_{c2} \sim$ 5 nm and it is comparable with the electron mean free path (see the Supplemental Material [35]), where $H_{c2} \sim 150$ kG for the field applied along the crystallographic c axis [37]. Therefore, it is safe to assume that the symmetry of the SC order parameter is not affected by the irradiation. Also, the irradiation did not affect the normal-state magnetization as shown in Fig. 1. However, the diamagnetic response below T_c in the field-cooled (FC) branch of the low-field magnetic susceptibility is noticeably suppressed after the ion irradiation (Fig. 3). This suppression is most likely caused by the trapping of the vortices by irradiation defects.

In the μSR experiments we focused on the irradiated samples. Prior to the ZF-μSR measurements we always performed TF measurements of each sample in the normal and SC states to estimate the amount and the relaxation rate of the background signal. The real part of the fast Fourier transform (FFT) is shown in Figs. 2(a)–2(c). The data analysis indicates that in all cases there is a contribution of a nonrelaxing background signal attributed to muons stopping outside of the sample and presumably in the cryostat walls. In the case of the sample with $x = 0.73$ (with mass $m_{s1} = 14.6$ mg) the background signal contribution was around 13% to 14% depending on the polarization mode and the sample mounting. However, in the case of the smaller sample ($m_{s2} = 10.5$ mg) with $x = 0.70$ a larger background signal ($\approx$30%) was determined. The obtained values of the background signal were used for analysis of the ZF data.

ZF measurements were performed under true zero-field conditions (with the compensated earth field) established after TF measurements at $T \sim 20$ K above T_c. Then the samples were cooled down to the base temperature of around 1.6 K. Each series of the measurements was performed with ascending temperature steps with a temperature stability better
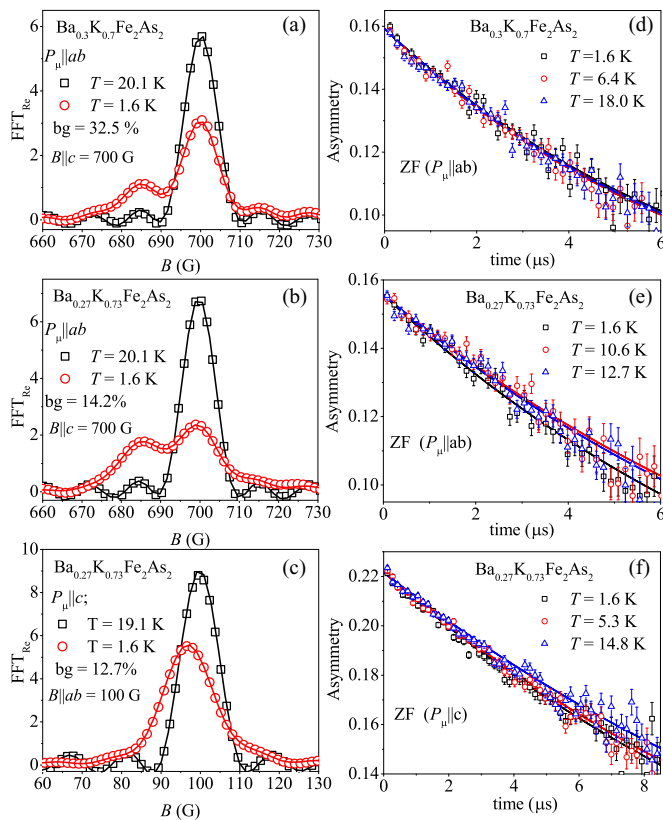
FIG. 2. The real part of the FFT of the transverse-field μSR time spectra obtained above and below T_c for irradiated $Ba_{1-x}K_xFe_2As_2$ samples: (a) $x = 0.70$, (b) $x = 0.73$ measured in the transverse polarization mode, and (c) $x = 0.73$ measured in the longitudinal polarization mode. The solid curves are fits to extract the background contribution to the μSR data. Representative ZF-μSR asymmetry time spectra of $Ba_{1-x}K_xFe_2As_2$ for (d) $x = 0.70$, (e) $x = 0.73$ measured in the transverse polarization mode, and (f) $x = 0.73$ measured in the longitudinal polarization mode. The solid curves are fits to Eq. (1), described in the text.

FIG. 3. (Left axis) Temperature dependence of the relaxation rate $\Delta\lambda = \lambda(T) - \lambda_0$ for $Ba_{1-x}K_xFe_2As_2$ samples: (a) $x = 0.73$, where $\lambda_0(T = 16 \text{ K}) = 0.085(2) \ \mu s^{-1}$ for $P_\mu \parallel ab$ and $0.054(1) \ \mu s^{-1}$ for $P_\mu \parallel c$, (b) $x = 0.70$, where $\lambda_0(T = 18 \text{ K}) = 0.131(3) \ \mu s^{-1}$ for $P_\mu \parallel ab$. The dashed curves are guides to the eyes. (Right axis) Temperature dependence of the volume susceptibility of the same samples before and after ion irradiation measured in a low magnetic-field $B \parallel ab = 5$ G applied after cooling in ZF, subsequent warming in the field, and cooling again in the same field (FC).

than 0.1 K. In the transversal polarization mode 3×10^6 counts per detector were measured at each temperature point, and 15×10^6 were measured in the longitudinal polarization mode. ZF-μSR asymmetry spectra of $Ba_{1-x}K_xFe_2As_2$ at different temperatures are shown in Figs. 2(d)–2(f). In the case of the sample with $x = 0.70$ the asymmetry spectra are essentially temperature independent. For the sample with $x = 0.73$ we observe a decrease of the relaxation rate with the increase in the temperature (see also Fig. 3). A similar behavior was observed for both polarization modes. To fit the asymmetry spectra the simplest possible model was used

$$A(t) = A_s(0)\exp[-\lambda/t] + A_{bg}, \qquad (1)$$

where $A_s(0)$ is the initial sample asymmetry, λ is the relaxation rate, and A_{bg} is the nonrelaxing background asymmetry obtained from TF measurements. The results of the fit by Eq. (1) are shown by the solid lines in Figs. 2(d)–2(f). The relaxation rate of our samples ($\lambda \approx 0.1 \ \mu s^{-1}$) for $P_\mu \parallel ab$ is similar to a total relaxation rate of the polycrystalline samples from Ref. [30] and slightly lower for $P_\mu \parallel c$ with $\lambda \approx 0.05 \ \mu s^{-1}$. However, in our case the relaxation shows an
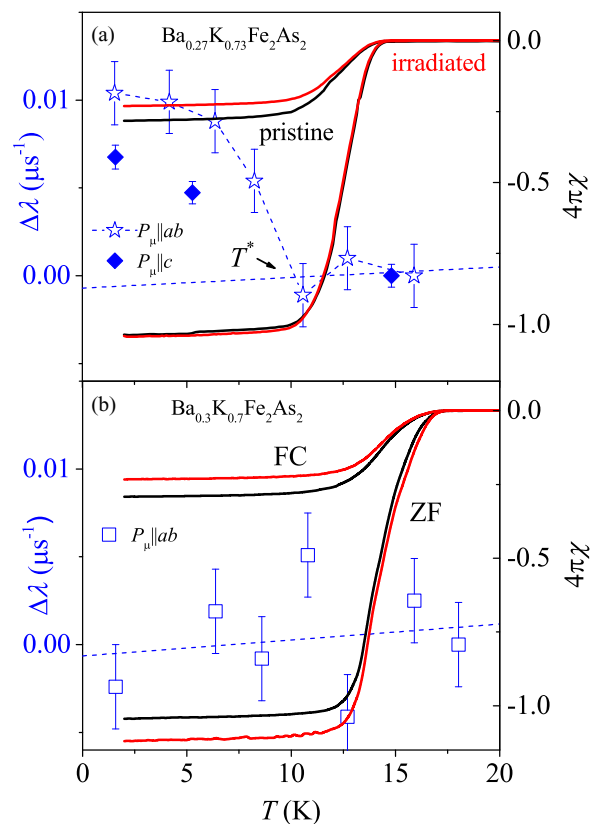
exponential behavior in contrast to the dominant Gaussian contribution in the polycrystalline samples attributed to a nuclear relaxation. Recently a weak exponential relaxation also was observed for optimally and slightly overdoped single crystals in Ref. [38]. A weaker relaxation rate for $P_\mu \parallel c$ of our crystals as compared to the polycrystalline samples cannot be attributed naively to an impurity contribution additional to the Gaussian relaxation due to randomly oriented nuclear moments. Therefore, the discrepancy between the relaxation behaviors of single crystals and the polycrystalline samples is not clear so far and requires further investigation.

The obtained temperature dependence of the relaxation rate $\Delta\lambda = \lambda(T) - \lambda_0$ for both samples together with the low-field susceptibility data are shown in Fig. 3, where λ_0 is the relaxation rate above T_c. $\Delta\lambda$ is enhanced at $T^* \sim 10 \text{ K} < T_c$ for the sample with $x = 0.73$ whereas it is nearly temperature independent for the sample with $x = 0.70$. The $\Delta\lambda$ value and the sharp enhancement are consistent with the appearance of weak magnetic fields due to impurity-induced currents in a BTRS SC state. Typically, $\Delta\lambda$, associated with this state, varies between 0.005 and 0.05 μs^{-1} for various superconductors [39–49]. In most of these superconductors

a time-reversal symmetry is broken already at T_c, which can be explained within a single-band approach. The known exception is $U_{1-x}Th_xBe_{13}$ where a BTRS state appears at the second $T_{c2} < T_{c1}$ [39]. So far the nature of the second transition in $U_{1-x}Th_xBe_{13}$ is under debate [50,51]. There are arguments in favor of a magnetic origin of this transition based on specific heat and thermal expansion measurements [50]. In contrast to $U_{1-x}Th_xBe_{13}$ for our samples we did not observe additional anomalies in the specific heat around T^* (see Fig. S3 in the Supplemental Material [35]). The lack of a clear anomaly imposes constraints on possible types of a BTRS state in $Ba_{1-x}K_xFe_2As_2$. In particular, an $s + id$ state proposed in Refs. [13,29] is unlikely. In this state both s- and d-order parameters are present with a relative phase shift of $\pm\pi/2$. These order parameters are weakly coupled due to different symmetries and therefore may appear at different temperatures. Hence, for an $s + id$ state one expects an anomaly in the specific heat at T^* similar to a transition at T_c. In contrast, the transition between an $s_\pm$ to an $s + is$ state may not result in a noticeable anomaly at T^* depending on the system parameters. In this case, gradual phase evolution of the gaps on different Fermi pockets and strong doping dependence of T^* can lead to a broad anomaly below T_c, which can hardly be distinguished from a specific heat of a multiband s-wave superconductor [26]. Also, according to calculations given in Ref. [23] the local internal fields associated with an $s + is$ state are expected to be in the range of $(10^{-8}–10^{-4})H_{c2} \sim 0.001$–10 G depending on the defect potential, whereas for an $s + id$ state the internal fields are about 10^3–10^5 times stronger. The experimental value of the average internal field of $\Delta\lambda/\gamma_\mu \sim 0.1$ Oe is too small for an $s + id$ state even considering the diluted irradiation defects only where $\gamma_\mu = 0.085 \ \mu s^{-1} G^{-1}$ is the muon gyromagnetic

ratio. Therefore, our data favor $s + is$ symmetry of the SC-order parameter in the $Ba_{1-x}K_xFe_2As_2$ system at $x \sim 0.7$. However, for an unambiguous discrimination between the $s + is$ and the $s + id$ SC states further investigations are necessary, such as systematic studies of the effect of ion irradiation on the value of the relaxation rate in the BTRS state. Additionally, the measurements of the local field distribution around nonmagnetic defects using a magnetic force microscope or a SC quantum interference device may help to determine directly the symmetry of the order parameter in the BTRS state [23].

Finally we conclude that ZF-μSR measurements of ion-irradiated moderately hole overdoped $Ba_{1-x}K_xFe_2As_2$ single crystals revealed a possible broken time-reversal symmetry in the SC state. This BTRS state forms below the bulk SC transition temperature T_c in qualitative agreement with theoretical predictions. Our as well as published data [30] suggest that the possible BTRS states occupy a very narrow region in between $x = 0.7$ and 0.8 in the phase diagram of $Ba_{1-x}K_xFe_2As_2$.

[1] P. J. Hirschfeld, M. M. Korshunov, and I. I. Mazin, Rep. Prog. Phys. **74**, 124508 (2011).

[2] K. Okazaki Y. Ota, Y. Kotani, W. Malaeb, Y. Ishida, T. Shimojima, T. Kiss, S. Watanabe, C.-T. Chen, K. Kihou, C. H. Lee, A. Iyo, H. Eisaki, T. Saito, H. Fukazawa, Y. Kohori, K. Hashimoto, T. Shibauchi, Y. Matsuda, H. Ikeda, H. Miyahara, R. Arita, A. Chainani, and S. Shin, Science **337**, 1314 (2012).

[3] F. Hardy R. Eder, M. Jackson, D. Aoki, C. Paulsen, T. Wolf, P. Burger, A. Böhmer, P. Schweiss, P. Adelmann, R. A. Fisher, and C. Meingasta, J. Phys. Soc. Jpn. **83**, 014711 (2014).

[4] D. Watanabe, T. Yamashita, Y. Kawamoto, S. Kurata, Y. Mizukami, T. Ohta, S. Kasahara, M. Yamashita, T. Saito, H. Fukazawa, Y. Kohori, S. Ishida, K. Kihou, C. H. Lee, A. Iyo, H. Eisaki, A. B. Vorontsov, T. Shibauchi, and Y. Matsuda, Phys. Rev. B **89**, 115112 (2014).

[5] T. Terashima, K. Kihou, K. Sugii, N. Kikugawa, T. Matsumoto, S. Ishida, C.-H. Lee, A. Iyo, H. Eisaki, and S. Uji, Phys. Rev. B **89**, 134520 (2014).

[6] Y. Ota, K. Okazaki, Y. Kotani, T. Shimojima, W. Malaeb, S. Watanabe, C.-T. Chen, K. Kihou, C. H. Lee, A. Iyo, H. Eisaki, T. Saito, H. Fukazawa, Y. Kohori, and S. Shin, Phys. Rev. B **89**, 081103(R) (2014).

[7] K. Hashimoto, A. Serafin, S. Tonegawa, R. Katsumata, R. Okazaki, T. Saito, H. Fukazawa, Y. Kohori, K. Kihou, C. H. Lee, A. Iyo, H. Eisaki, H. Ikeda, Y. Matsuda, A. Carrington, and T. Shibauchi, Phys. Rev. B **82**, 014526 (2010).

[8] J. P. Reid, M. A. Tanatar, A. Juneau-Fecteau, R. T. Gordon, S. R. de Cotret, N. Doiron-Leyraud, T. Saito, H. Fukazawa, Y. Kohori, K. Kihou, C. H. Lee, A. Iyo, H. Eisaki, R. Prozorov, and L. Taillefer, Phys. Rev. Lett. **109**, 087001 (2012).

[9] M. Abdel-Hafiez, V. Grinenko, S. Aswartham, I. Morozov, M. Roslova, O. Vakaliuk, S. Johnston, D. V. Efremov, J. van den Brink, H. Rosner, M. Kumar, C. Hess, S. Wurmehl, A. U. B. Wolter, B. Büchner, E. L. Green, J. Wosnitza, P. Vogt, A. Reifenberger, C. Enss, M. Hempel, R. Klingeler, and S.-L. Drechsler, Phys. Rev. B **87**, 180507(R) (2013).

[10] H. Kim, M. A. Tanatar, Yong Liu, Z. C. Sims, C. Zhang, P. Dai, T. A. Lograsso, and R. Prozorov, Phys. Rev. B **89**, 174519 (2014).

[11] V. Grinenko, D. V. Efremov, S. L. Drechsler, S. Aswartham, D. Gruner, M. Roslova, I. Morozov, K. Nenkov, S. Wurmehl, A. U. B. Wolter, B. Holzapfel, and B. Büchner, Phys. Rev. B **89**, 060504(R) (2014).

[12] S. Graser, T. A. Maier, P. J. Hirschfeld, and D. J. Scalapino, New J. Phys. **11**, 025016 (2009).

[13] R. Thomale, C. Platt, W. Hanke, J. Hu, and B. A. Bernevig, Phys. Rev. Lett. **107**, 117001 (2011).

[14] S. Maiti, M. M. Korshunov, T. A. Maier, P. J. Hirschfeld, and A. V. Chubukov, Phys. Rev. B **84**, 224505 (2011).

[15] S. Maiti and A. V. Chubukov, Phys. Rev. B **87**, 144511 (2013).

[16] M. Marciani, L. Fanfarillo, C. Castellani, and L. Benfatto, Phys. Rev. B **88**, 214508 (2013).

[17] N. Xu, P. Richard, X. Shi, A. van Roekeghem, T. Qian, E. Razzoli, E. Rienks, G.-F. Chen, E. Ieki, K. Nakayama, T. Sato, T. Takahashi, M. Shi, and H. Ding, Phys. Rev. B **88**, 220508(R) (2013).

[18] C. H. Lee, K. Kihou, J. T. Park, K. Horigane, K. Fujita, F. Wasser, N. Qureshi, Y. Sidis, J. Akimitsu, and M. Braden, Sci. Rep. **6**, 23424 (2016).

[19] S. L. Bud'ko, M. Sturza, D. Y. Chung, M. G. Kanatzidis, and P. C. Canfield, Phys. Rev. B **87**, 100509(R) (2013).

[20] F. Hardy, A. E. Böhmer, L. de Medici, M. Capone, G. Giovannetti, R. Eder, L. Wang, M. He, T. Wolf, P. Schweiss, R. Heid, A. Herbig, P. Adelmann, R. A. Fisher, and C. Meingast, Phys. Rev. B **94**, 205113 (2016).

[21] S. Maiti, M. M. Korshunov, and A. V. Chubukov, Phys. Rev. B **85**, 014511 (2012).

[22] S. Maiti, M. Sigrist, and A. Chubukov, Phys. Rev. B **91**, 161102 (2015).

[23] S.-Z. Lin, S. Maiti, and A. Chubukov, Phys. Rev. B **94**, 064519 (2016).

[24] V. Stanev and Z. Tesanović, Phys. Rev. B **81**, 134522 (2010).

[25] J. Garaud and E. Babaev, Phys. Rev. Lett. **112**, 017003 (2014).

[26] M. Silaev, J. Garaud, and E. Babaev, Phys. Rev. B **95**, 024517 (2017).

[27] C. Platt, R. Thomale, C. Honerkamp, S.-C. Zhang, and W. Hanke, Phys. Rev. B **85**, 180502(R) (2015).

[28] J. Boeker, P. A. Volkov, K. B. Efetov, and I. Eremin, arXiv:1704.08185.

[29] W.-C. Lee, S.-C. Zhang, and C. Wu, Phys. Rev. Lett. **102**, 217002 (2009).

[30] Z. L. Mahyari, A. Cannell, C. Gomez, S. Tezok, A. Zelati, E. V. L. de Mello, J.-Q. Yan, D. G. Mandrus, and J. E. Sonier, Phys. Rev. B **89**, 020502 (2014).

[31] M. B. Schilling, A. Baumgartner, B. Gorshunov, E. S. Zhukova, V. A. Dravin, K. V. Mitsen, D. V. Efremov, O. V. Dolgov, K. Iida, M. Dressel, and S. Zapf, Phys. Rev. B **93**, 174515 (2016).

[32] https://www.psi.ch/smus/gps

[33] A. Suter and B. M. Wojek, Phys. Procedia **30**, 69 (2012).

[34] K. Kihou, T. Saito, K. Fujita, S. Ishida, M. Nakajima, K. Horigane, H. Fukazawa, Y. Kohori, S. Uchida, J. Akimitsu, A. Iyo, C.-H. Lee, and H. Eisaki, J. Phys. Soc. Jpn. **85**, 034718 (2016).

[35] See Supplemental Material at http://link.aps.org/supplemental/10.1103/PhysRevB.95.214511 for additional x-ray, electrical resistivity and specific heat data for the $B_{1-x}K_xFe_2As_2$ single crystals used in our μSR experiments.

[36] L. Fang, Y. Jia, C. Chaparro, G. Sheet, H. Claus, M. A. Kirk, A. E. Koshelev, U. Welp, G. W. Crabtree, W. K. Kwok, S. Zhu, H. F. Hu, J. M. Zuo, H.-H. Wen, and B. Shen, Appl. Phys. Lett. **101**, 012601 (2012).

[37] Y. Liu, M. A. Tanatar, W. E. Straszheim, B. Jensen, K. W. Dennis, R. W. McCallum, V. G. Kogan, R. Prozorov, and T. A. Lograsso, Phys. Rev. B **89**, 134504 (2014).

[38] B. P. P. Mallett, C. N. Wang, P. Marsik, E. Sheveleva, M. Yazdi-Rizi, J. L. Tallon, P. Adelmann, T. Wolf, and C. Bernhard, Phys. Rev. B **95**, 054512 (2017).

[39] R. H. Heffner, J. L. Smith, J. O. Willis, P. Birrer, C. Baines, F. N. Gygax, B. Hitti, E. Lippelt, H. R. Ott, A. Schenck, E. A. Knetsch, J. A. Mydosh, and D. E. MacLaughlin, Phys. Rev. Lett. **65**, 2816 (1990).

[40] G. M. Luke, Y. Fudamoto, K. M. Kojima, M. I. Larkin, J. Merrin, B. Nachumi, Y. J. Uemura, Y. Maeno, Z. Q. Mao, Y. Mori, H. Nakamura, and M. Sigrist, Nature (London) **394**, 558 (1998).

[41] Y. Aoki, A. Tsuchiya, T. Kanayama, S. R. Saha, H. Sugawara, H. Sato, W. Higemoto, A. Koda, K. Ohishi, K. Nishiyama, and R. Kadono, Phys. Rev. Lett. **91**, 067003 (2003).

[42] A. D. Hillier, J. Quintanilla, and R. Cywinski, Phys. Rev. Lett. **102**, 117007 (2009).

[43] A. Maisuradze, W. Schnelle, R. Khasanov, R. Gumeniuk, M. Nicklas, H. Rosner, A. Leithe-Jasper, Y. Grin, A. Amato, and P. Thalmeier, Phys. Rev. B **82**, 024524 (2010).

[44] L. Shu, W. Higemoto, Y. Aoki, A. D. Hillier, K. Ohishi, K. Ishida, R. Kadono, A. Koda, O. O. Bernal, D. E. MacLaughlin, Y. Tunashima, Y. Yonezawa, S. Sanada, D. Kikuchi, H. Sato, H. Sugawara, T. U. Ito, and M. B. Maple, Phys. Rev. B **83**, 100504(R) (2011).

[45] A. D. Hillier, J. Quintanilla, B. Mazidian, J. F. Annett, and R. Cywinski, Phys. Rev. Lett. **109**, 097001 (2012).

[46] P. K. Biswas, H. Luetkens, T. Neupert, T. Stürzer, C. Baines, G. Pascua, A. P. Schnyder, M. H. Fischer, J. Goryo, M. R. Lees, H. Maeter, F. Brückner, H.-H. Klauss, M. Nicklas, P. J. Baker, A. D. Hillier, M. Sigrist, A. Amato, and D. Johrendt, Phys. Rev. B **87**, 180503(R) (2013).

[47] R. P. Singh, A. D. Hillier, B. Mazidian, J. Quintanilla, J. F. Annett, D. McK. Paul, G. Balakrishnan, and M. R. Lees, Phys. Rev. Lett. **112**, 107002 (2014).

[48] J. Zhang, D. E. MacLaughlin, A. D. Hillier, Z. F. Ding, K. Huang, M. B. Maple, and L. Shu, Phys. Rev. B **91**, 104523 (2015).

[49] J. A. T. Barker, D. Singh, A. Thamizhavel, A. D. Hillier, M. R. Lees, G. Balakrishnan, D. McK. Paul, and R. P. Singh, Phys. Rev. Lett. **115**, 267001 (2015).

[50] F. Kromer, R. Helfrich, M. Lang, F. Steglich, C. Langhammer, A. Bach, T. Michels, J. S. Kim, and G. R. Stewart, Phys. Rev. Lett. **81**, 4476 (1998).

[51] J. E. Sonier, R. H. Heffner, D. E. MacLaughlin, G. J. Nieuwenhuys, O. Bernal, R. Movshovich, P. G. Pagliuso, J. Cooley, J. L. Smith, and J. D. Thompson, Phys. Rev. Lett. **85**, 2821 (2000).